Chapter 18
Application of Layered Double Hydroxides (LDHs) in Photocatalysis

Shoji Iguchi, Kentaro Teramura, Saburo Hosokawa, and Tsunehiro Tanaka

18.1 Fundamentals of Layered Double Hydroxides (LDHs)

Layered double hydroxides (LDHs), also called hydrotalcite-like compounds, are natural and/or synthetic anionic clay materials. The term LDH was coined in the early works of Feithnecht, who named them "Doppelschichtstruktruren" (i.e., double layer structures), presuming a structure with intercalated hydroxide layers. This hypothesis was refuted many years later on the basis of single-crystal X-ray diffraction (XRD) analysis, which showed that LDHs consist of positively charged two-dimensional (2D) sheets, with all the cations located in the same layer, and the charge-compensating anions and water molecules in the interlayer region (Fig. 18.1) [1, 2]. It is known that the parent material of these anionic clays is the natural mineral hydrotalcite, which has the formula $Mg_6Al_2(OH)_{16}CO_3{\cdot}4H_2O$. The general formula of LDHs is

$$\left[M^{2+}_{1-x}M^{3+}_{x}\left(OH\right)_2\right]^{x+}\left(A^{n-}_{x/n}\right)\cdot mH_2O$$

where M^{2+} and M^{3+} are divalent and trivalent cations, respectively; x represents the molar ratio of $M^{3+}/(M^{2+} + M^{3+})$, whereas A^{n-} is the interlayer anion of valence n. The natures of M^{2+}, M^{3+}, x, and A^{n-} might vary over a wide range, thus giving rise to a large number of isostructural materials, with variegated physical and chemical properties. The value of x to form a pure LDH phase is reported to range from 0.2 to 0.4. When the x value is outside of this range, hydroxides or other compounds are formed as impurity phases. The divalent cations (M^{2+}=Fe^{2+}, Co^{2+}, Ni^{2+}, Cu^{2+}, Zn^{2+}, Mn^{2+}, Cd^{2+}, and Ca^{2+}) and the trivalent cations (M^{3+}=Co^{3+}, Fe^{3+}, Mn^{3+}, Ga^{3+}, Cr^{3+}, In^{3+}, V^{3+}, Y^{3+}, La^{3+}) form LDHs through fully or partially replacing Mg^{2+} or Al^{3+} of the brucite-like layer of

S. Iguchi • K. Teramura (✉) • S. Hosokawa • T. Tanaka (✉)
Department of Molecular Engineering, Graduate School of Engineering, Kyoto University, Kyotodaigaku Katsura, Nishikyo-ku, Kyoto 615-8510, Japan
e-mail: teramura@moleng.kyoto-u.ac.jp; tanakat@moleng.kyoto-u.ac.jp

H. Yamashita, H. Li (eds.), *Nanostructured Photocatalysts*, Nanostructure Science and Technology, DOI 10.1007/978-3-319-26079-2_18

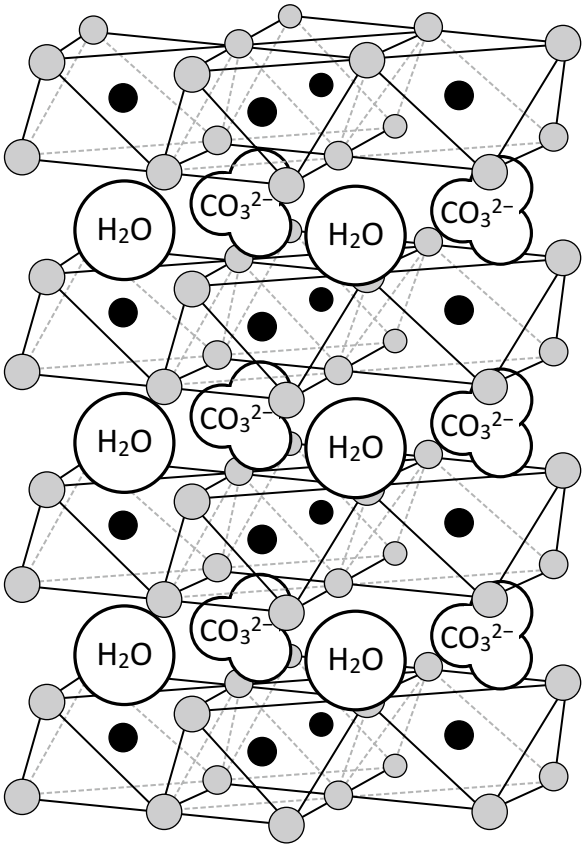

Fig. 18.1 Schematic representation of the structure of LDHs containing CO_3^{2-} as interlayer anions

hydrotalcite [3]. In addition, tetravalent cations, such as Ti^{4+} [4], Zr^{4+} [5], and Sn^{4+} [6], also incorporate into the brucite-like layer, whereas some evidences reveal that M^{4+} cations form amorphous oxide particles instead of incorporating in the brucite-like layer. Multi-metal cations can be simultaneously incorporated into the brucite-like layer to prepare multi-component LDHs, provided x is in the correct range. The most common anion found in naturally occurring LDHs is carbonate (CO_3^{2-}), which shows a high affinity for the interlayer in a series of LDHs. In fact, various kinds of charge-compensating anions may be incorporated into the interlayer, namely inorganic anions (NO_3^-, SO_4^{2-}, halides, oxyanions, silicates, etc.), polyoxometalate anions ($Mo_7O_{24}^{6-}$, $W_7O_{24}^{6-}$, $V_{10}O_{28}^{6-}$, $PMo_{12}O_{40}^{3-}$, $PW_{12}O_{40}^{3-}$, etc.), complex anions (porphyrin complexes, phthalocyanine complexes, $Fe(CN)_6^{4-}$/$Fe(CN)_6^{3-}$), and organic anions (carboxylates, dicarboxylates, alkylsulfates, alkanesulfates, etc.) [3].

LDHs are widely used as basic materials for CO_2 capture and storage [7], removal of organic and inorganic anions from the aqueous solution [8–10], and base-catalyzed reactions [11]. Ebitani et al. reported that Mg–Al LDHs catalyze the aldol condensation of carbonyl compounds in an aqueous solution because their surface base sites show the property of high water tolerance [12], indicating that basic sites of LDHs and their derivatives may function in the presence of water.

18.2 Preparation

As reviewed by Reichle [13] and Cavani et al. [1], various preparation methods of LDHs have been developed. The optimum conditions, e.g., atmosphere, temperature, pH during the precipitation, concentration of precursor solution, aging procedure, etc., should be chosen in accordance with the kinds of metal components constituting the hydroxide sheets.

Co-precipitation method: LDHs are traditionally synthesized by co-precipitation from aqueous solution. The most common procedure is the constant-pH co-precipitation process, wherein the mixed aqueous solution of the metal components and the base solution (normally, an aqueous solution of NaOH) are added simultaneously to an aqueous solution of Na_2CO_3 to maintain the suspension at a stable pH. In the so-called variable pH co-precipitation process, LDHs containing CO_3^{2-} as interlayer anions are prepared by gradually adding the aqueous solution containing the metal cations to the aqueous solution of Na_2CO_3 until the suspension reaches a specified pH. As necessary, the aqueous solution of NaOH is then used to maintain the pH until the precipitation is completed. In both processes, the resulting suspension is stirred at a certain temperature as an aging for varying periods of time, and then collected by filtration. The filter cake is washed with pure water and is then dried [14].

Hydrothermal synthesis: Hydrothermal treatment is usually applied to obtain well-crystallized LDHs with large platelets. Homogeneous co-precipitation method under hydrothermal conditions is an advanced technique to synthesize well-defined LDH particles. Ogawa et al., for example, reported the following procedure: an aqueous solution containing urea and salts of the metal components mixed in a certain ratio were transferred into an autoclave and heated at 393 K for 24 h. After cooling to room temperature, the solid precipitate was collected and washed with deionized water. The pH of the solution changed from 3.4 to 8.4 during the course of the reaction, through the hydrolysis of urea [15]. We synthesized various kinds of LDHs via co-precipitation method combined with hydrothermal treatment as follows: after constant pH co-precipitation process at room temperature, the resulting suspension is transferred to a stainless steel autoclave with an inner Teflon vessel, and aged under hydrothermal conditions at 383 K. The resultant solid is collected by filtration and washed with 1.0 L of ultrapure water, and then dried at 383 K in air [16].

Rehydration: Since atmospheric CO_2 is incorporated into the structure of LDH with high affinity, most synthesized LDHs contain CO_3^{2-} as interlayer anions or as surface-adsorbed species. The rehydration process (also called the reconstruction process), based on the "memory effect," is necessary to obtain carbonate-free LDHs. As-prepared LDH is calcined at over 773 K in air or in an inert gas atmosphere to produce the mixed oxide via decomposition of its characteristic layered structure. The resulting mixed oxide is immersed in decarbonated water at room temperature for several hours under an inert gas atmosphere to yield rehydrated LDH, during which the layer structures of the hydroxide sheets are reconstructed and the charge-compensating CO_3^{2-} anions are replaced by OH^- anions [17]. Medina et al. argued that the rehydrated Mg–Al LDH that have active hydroxyl groups located near the edges of the platelets exhibits high performance in aldol condensations [18].

18.3 Characterization

XRD patterns: The most common technique for characterizing LDH structures is XRD. However, as the materials are often poorly crystallized, the diffraction patterns are broad and asymmetric, and hence difficult to analyze. The sharp diffraction peaks at low angle are assigned to the (003) and (006) phase reflections. These peaks are related to intervals of each hydroxide sheet and the distance from the hydroxide sheets to the interlayer anions, respectively, indicating that corresponding peaks are influenced by the interlayer anion size, the ratio of M^{2+}/M^{3+}, and the degree of hydration. The other intense peak around $2\theta = 60°$ is indexed as a (110) phase with respect to the hexagonal axes. This reflection is independent of the kind of layer stacking and can therefore be utilized for the calculation of the parameter a as $2d_{(110)}$. The value of a should depend on the nature of the metal cations of the hydroxide sheets (the ionic radii of the cations) and the ratio of the metal components (Fig. 18.2a) [1].

Fourier-transform Infrared (FT-IR) spectroscopy: FT-IR spectroscopy is useful in identifying the presence of interlayer anions of LDHs and their derivatives. Information can be obtained about the type of bonds formed by the anions and their orientations. The adsorption at 3500–3600 cm^{-1} is attributed to the hydrogen bonding stretching vibration of the OH group of the hydroxide sheets. A shoulder may be present at ~3000 cm^{-1}, assigned to hydrogen bonding between H_2O and the interlayer anions. The intensity and the position of this band depend on the type of anions and the amount of water in the interlayer. The main absorption bands corresponding to interlayer anions are observed between 1000 and 1800 cm^{-1}. The peak due to vibration of the interlayer carbonates (chelating or bridging bidentate) appeared at 1370 cm^{-1}. The vibration at 1515 cm^{-1} is ascribed to a reduction in the symmetry, caused by monodentate carbonates interacting with Mg^{2+} [1, 18]. Medina et al., in the case of Mg–Al LDH, noticed that a significant amount of carbonates remain after the calcination/rehydration process due to the high affinity of carbonates to LDHs [18].

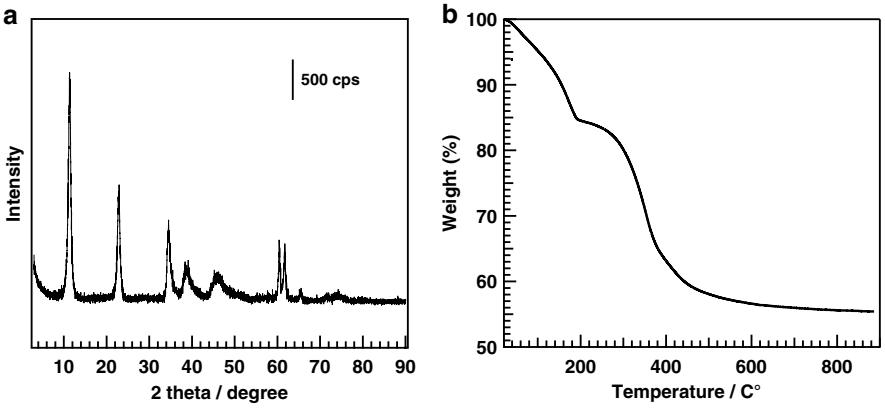

Fig. 18.2 (**a**) XRD pattern of Mg–Al LDH measured by using Cu K_α radiation, (**b**) TG curve of Mg–Al LDH. Both of them are the original data from the authors of this chapter

Thermogravimetry: Their thermal behavior reflects many features of LDHs, such as the ratio of M^{2+}/M^{3+}, kinds of interlayer anions, and degree of hydration. LDHs exhibit characteristic two-step weight loss with increasing temperature in the TG curve. The first step, at less than 500 K, is due to desorption of water molecules present on the surface and in the interlayer without the decomposition of the layered structure. The second step, above 500 K, is caused by collapse of the layered structure accompanied by the dehydration of hydroxyl groups and desorption of the charge-compensating interlayer anions (Fig. 18.2b).

In addition, the densities and strengths of basic sites in LDHs and their derivatives are determined by temperature-programmed desorption (TPD) profiles combined with the results of FT-IR spectra and the thermogravimetric profiles. Scanning electron microscopy (SEM) images typically reveal the morphology of the synthesized LDHs. The characteristic layered structures and the platelet morphology are clearly observed.

18.4 Application to Photocatalytic Reactions

18.4.1 Degradation of Organic Compounds

The photocatalytic elimination of toxic organic pollutants using visible light has been extensively studied for two decades. From the perspectives of environmental concerns and energy shortages, it is necessary to develop a novel photocatalyst, which can effectively utilize renewable and clean solar energy. Although the band edge of TiO_2-based materials (such as $TiO_{2-x}N_x$) significantly shifts toward the visible region, their photoelectronic transition efficiencies are low due to inherent light absorption properties of these materials. Aiming to obtain a novel photocatalyst with large surface area and high crystallinity, ordered layer photocatalysts have been paid great attentions [19].

Zn-containing LDHs (Zn–M LDHs) are widely used as photocatalysts for the degradation of organic compounds. Shao et al. reported that as-prepared Zn–Ti LDH, with a low band gap of ca. 3.1 eV exhibited significant photocatalytic activity for the degradation of Methylene blue under visible light irradiation; a level of activity was much higher than those of ZnO and TiO_2. Furthermore, Zn–Ti LDH is stable through five repeated application cycles with nearly constant photodecomposition percentage, indicating that Zn–Ti LDH does not deactivate during the photocatalytic process [20]. Xia et al. demonstrated the photocatalytic degradation of Rhodamine B (RB) under visible light irradiation using a series of Zn–M LDH (M = Al, Fe, Ti, and FeTi). The degradation rates of RB for all four of the LDHs are over 50 % after the photoirradiation for 60 min, in the following order: Zn–Ti ≈ Zn–Al > Zn–Fe–Ti > Zn–Fe LDHs. Thermal regeneration of the Zn–Ti LDH utilized for RB degradation was feasible for at least three cycles, indicating that the structural stability of this material is sufficient to use it repeatedly as a photocatalyst for the degradation of RB [21]. In addition, various Zn–M LDHs, such as Zn–Cr [22],

Ag-loaded Zn–Cr [23], Pt-loaded Zn–Ti [24], Zn–Bi [25], and Mg–Zn–In LDH [19] have been reported as photocatalysts for the decomposition of organic compounds. On the other hand, metal oxides/LDH composites have been also reported to show similar activity for these photocatalytic reactions. Valente et al. presented the preparation of CeO_2 supported by Mg–Al LDH and their photocatalytic activities for the degradation of phenol and phenol-derivatives [26]. The photocatalytic systems for the degradation of organic dyes and compounds using TiO_2/Mg–Al LDH [27], ZnO/Mg–Al LDH [28], SnO_2/Mg–Al LDH [29], Fe_3O_4/Zn–Cr LDH [30], and $(W_7O_{24})^{6-}$-intercalated Mg–Al LDH [31] were also demonstrated.

18.4.2 Water Splitting

Since Honda and Fujishima found the photoelectrochemical water-splitting system using TiO_2 as a photoanode, various inorganic materials have been applied to catalyze the photocatalytic splitting of water. As brucite-like hydroxide sheets of LDHs can incorporate various kinds of metal cations to achieve the characteristic light absorption properties, some LDHs have recently attracted attention for their potential as new visible-light-responsive photocatalysts. LDHs are sometimes fabricated via a homogeneous precipitation method using urea and/or other amine compounds, as mentioned above. Organic residues cannot be removed by the mild heat treatment that enables LDHs to maintain their characteristic layered structure. Hence, it should be noted that such organic contaminants might influence photocatalytic activities.

García et al. reported that semiconductor materials based on three kinds of Zn^{2+}-containing LDHs (Zn–Cr, Zn–Ti, and Zn–Ce LDH) show photocatalytic activity for O_2 evolution from water under visible light irradiation, in the presence of $AgNO_3$ as a sacrificial reagent. As shown in Fig. 18.3, a certain amount of O_2 was evolved under visible light irradiation using Zn–Cr LDH as the photocatalyst; furthermore, once the photocatalytic reaction rate tends to slow down, addition of $AgNO_3$ reactivates the formation of O_2. It is indicated that the reason for the cessation in O_2 evolution is the lack of the sacrificial reagent, and not deactivation or corrosion of the catalyst. It should also be noted that the overall efficiency of the Zn–Cr LDH for O_2 generation under visible light irradiation is 1.6 times higher than that of a WO_3 photocatalyst under the same reaction conditions [4]. Wei et al. published a visible-light-responsive photocatalyst fabricated by anchoring Ni–Ti LDH to the surface of reduced graphene oxide sheets (RGO) that displays good activity for the photocatalytic O_2 evolution. The generation rates of O_2 over Ni–Ti LDH/RGO composites are much larger compared to bare Ni–Ti LDH and RGO, respectively; that is, the combination of Ni–Ti LDH and RGO significantly enhances the photocatalytic activity [32].

Wei et al. also reported a photocatalytic H_2 production system using various LDHs as photocatalysts that contain highly dispersed TiO_6 units. Ni–Ti, Zn–Ti, and Mg–Al–Ti LDH show photocatalytic activity for H_2 evolution using lactic acid as a sacrificial electron donor. In particular, Zn–Ti LDH, which contains highly dispersed TiO_6 units, displays a production rate 18 times higher than that of $K_2Ti_4O_9$, which

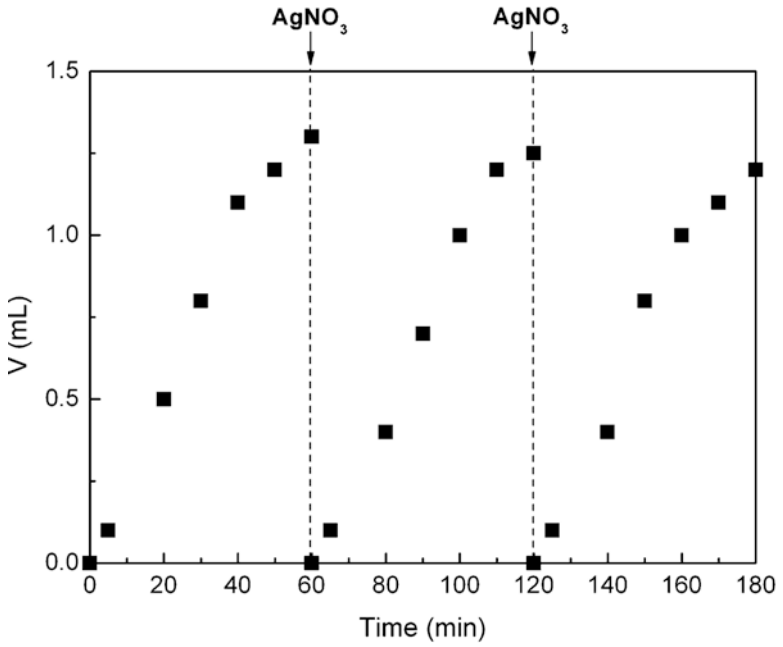

Fig. 18.3 Volume of O_2 formed vs. irradiation time in three consecutive cycles in which additional amounts of $AgNO_3$ have been added every 60 min. Reprinted with permission from Journal of the American Chemical Society, 2009, *131*, 13833. Copyright (2009) American Chemical Society

contains highly aggregated TiO_6 octahedra [33]. On the other hand, Xu et al. demonstrated photocatalytic H_2 evolution with Rose bengal (RBdye) and Pt nanoparticles (photosensitizers) fixed on Mg–Al LDH (co-catalyst). A self-assembled RBdye–LDH–Pt system produces H_2 from water that contains Triethanolamine (TEOA) as a sacrificial reagent; the amount is a few times greater than that of the RBdye–Pt (without LDH) system. Pt nanoparticles on Mg–Al LDH can be used repeatedly, and the total turnover number after six runs for the RBdye–LDH–Pt system is calculated to be 304, based on Pt. Photocatalytic water splitting has many advantages: (1) immobilizing the dye photosensitizer for suppressed self-quenching, (2) close arrangement between photosensitizer molecules and co-catalyst nanoparticles for efficient electron transfer, (3) formation of well-dispersed co-catalyst nanoparticles on the support surface, and (4) easy recycling of the expensive co-catalyst [34].

18.4.3 CO_2 Conversion

Photocatalytic conversion of CO_2 to valuable compounds is one of the promising methods to create a sustainable carbon-cycling system. The CO_2 molecules adsorbed on the surface of photocatalysts should be converted into active species that can be

easily reduced by photogenerated electrons. Therefore, solid base materials are suitable candidates to construct the photocatalytic system for CO_2 conversion [35]. In the last 5 years, several research groups have demonstrated the photocatalytic conversion of CO_2 using synthetic LDHs. Izumi et al. reported that Cu^{2+}-containing LDH photocatalysts show activity for CO_2 conversion using H_2 as the reductant, and CO and methanol are evolved as the reduction products of CO_2. In their system, $[Zn_3Ga(OH)_8]^+_2[Cu(OH)_4]^{2-}{\cdot}mH_2O$ and $[Zn_{1.5}Cu_{1.5}Ga(OH)_8]^+_2(CO_3)^{2-}{\cdot}mH_2O$ are used as photocatalysts, and the former shows higher activity than the latter for methanol formation as the reduction product of CO_2. Cu^{2+} species, in the interlayer for the former and in the inlayer for the latter, are considered active sites for CO_2 conversion under the irradiation [36–38]. Katsumata et al. also exhibited that noble-metal (Pt, Pd, and Au)-loaded Zn–Cr LDHs are active for the photocatalytic conversion of CO_2 to CO under UV irradiation. Since CO is not detected under visible light irradiation, it is concluded that photocatalytic conversion of CO_2 does not occur by absorption of the 410- and 570-nm peaks attributed to *d–d* transition [39].

We have published papers concerned with the photocatalytic system using various kinds of LDHs for CO_2 conversion. We reported a series of synthetic M^{2+}–M^{3+} LDHs ($M^{2+} = Mg^{2+}$, Ni^{2+}, and Zn^{2+}; $M^{3+} = Al^{3+}$, Ga^{3+}, and In^{3+}) that show activity toward the photocatalytic conversion of CO_2 in water [40]. As shown in Fig. 18.4, the use of Ni–Al LDH as a photocatalyst enabled us to achieve maximum conversion of CO_2 to CO with high selectivity, because it produces less H_2 as a reduction product of H^+ derived from water than other LDHs [16]. On the other hand, other LDHs such as Mg–In LDH and Ni–In LDH, both of which contain In^{3+} as a triva-

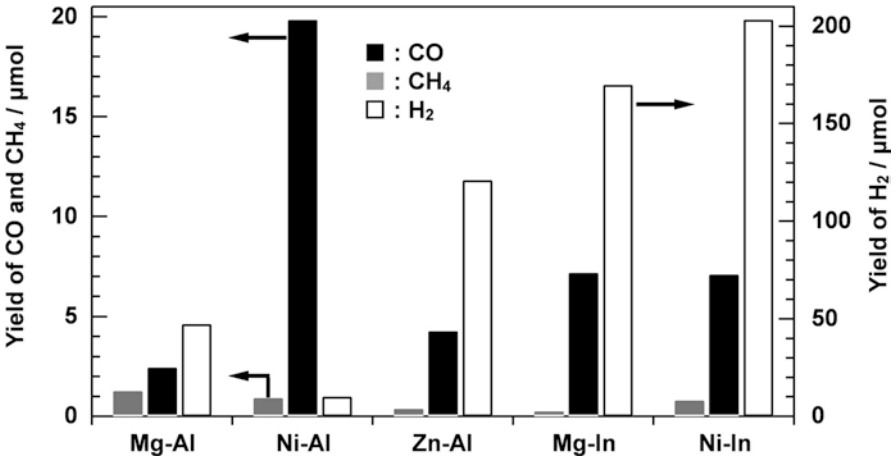

Fig. 18.4 The amount of products evolved in the photocatalytic conversion of CO_2 in H_2O over various M^{2+}–M^{3+} LDH after 8 h of photoirradiation. Black bar: CO, gray bar: CH4, white bar: H_2, $M^{2+}/M^{3+} = 3$, photocatalyst weight: 500 mg, CO_2: 7.7 mmol, H_2O: 350 mL, light source: 400 W Hg lamp. Reprinted from Catalysis Today, 251, Shoji Iguchi, Kentaro Teramura, Saburo Hosokawa, and Tsunehiro Tanaka, Photocatalytic conversion of CO_2 in an aqueous solution using various kinds of layered double hydroxides, 140, Copyright (2015), with permission from Elsevier

lent cation, increase the H_2 production, a less preferable condition. This led us to conclude that Ni–Al LDHs offer suitable surface properties for selective photocatalytic conversion of CO_2 in water. In addition, we found that the addition of NaCl into the reaction solution obviously improved the photocatalytic conversion of CO_2 to CO. More than twice amount of CO was evolved in an aqueous solution of NaCl (0.1 M) after 8 h of photoirradiation as compared to that in a pure water. Simultaneously, the addition of NaCl suppressed the H_2 formation as a reduction product of H^+. Accordingly, the selectivity toward CO evolution was advanced by the addition of NaCl to the reaction solution. Furthermore, NaCl was no exception as an additive, and that other chloride salts such as KCl, CsCl, $MgCl_2$, and $CaCl_2$ influenced the selectivity toward CO evolution to a similar extent, indicating that the presence of Cl^- in the reaction solution promoted the photocatalytic conversion of CO_2 regardless of the nature of the counter cation. The products CO, H_2, and HClO are formed under photoirradiation as a reduction product of CO_2 and H^+, and as an oxidation product of Cl^-, respectively. It should be possible to detect HClO selectively by using a *N,N′*-dimethyl-*p*-phenylenediamine (DPD) test due to the strong oxidation power of HClO. We conclude that the photogenerated holes during the photocatalytic reaction oxidize the reducing agent Cl^- to Cl_2, which is immediately converted into HClO in the presence of water [41].

References

1. Cavani F, Trifirò F, Vaccari A (1991) Hydrotalcite-type anionic clays: preparation, properties and applications. Catal Today 11:173–301
2. Hoyo CD (2007) Layered double hydroxides and human health: an overview. Appl Clay Sci 36:103–121
3. Xu ZP, Zhang J, Adebajo MO, Zhang H, Zhou C (2011) Catalytic applications of layered double hydroxides and derivatives. Appl Clay Sci 53:139–150
4. Silva CG, Bouizi Y, Fornés V, García H (2009) Layered double hydroxides as highly efficient photocatalysts for visible light oxygen generation from water. J Am Chem Soc 131:13833–13839
5. Saber O (2007) Preparation and characterization of a new nano layered material, Co–Zr LDH. J Mater Sci 42:9905–9912
6. Saber O, Tagaya H (2003) Preparation and intercalation reaction of Zn–Sn LDH and Zn–Al–Sn LDH. J Porous Mater 10:83–91
7. Ram Reddy MK, Xu ZP, Lu GQ, Diniz da Costa JC (2006) Layered double hydroxide for CO_2 capture: structure evolution and regeneration. Ind Eng Chem Res 45:7504–7509
8. Goh KH, Lim TT, Dong Z (2008) Application of layered double hydroxides for removal of oxyanions: a review. Wat Res 42:1343–1368
9. Das J, Patra BS, Baliarsingh N, Parida KM (2006) Adsorption of phosphate by layered double hydroxides in aqueous solutions. Appl Clay Sci 32:252–260
10. Goswamee RL, Sengupta P, Bhattacharyya KG, Dutta DK (1998) Adsorption of Cr (VI) in layered double hydroxides. Appl Clay Sci 13:21–34
11. Sels BF, De Vos DE, Jacobs PA (2001) Hydrotalcite-like anionic clays in catalytic organic reactions. Catal Rev 43:443–488
12. Ebitani K, Motokura K, Mori K, Mizugaki T, Kaneda K (2006) Reconstructed hydrotalcite as a highly active heterogeneous base catalyst for carbon-carbon bond formations in the presence of water. J Org Chem 71:5440–5447

13. Reichle WT (1986) Synthesis of anionic clay minerals (mixed metal hydroxides, hydrotalcite). Solid State Ionics 22:135–141
14. Evans DG, Duan X (2006) Preparation of layered double hydroxides and their applications as additives in polymers, as precursors to magnetic materials and in biology and medicine. Chem Commun 42:485–496
15. Ogawa M, Kaiho H (2002) Homogeneous precipitation of uniform hydrotalcite particles. Langmuir 18:4240–4242
16. Iguchi S, Teramura K, Hosokawa S, Tanaka T (2014) Photocatalytic conversion of CO_2 in an aqueous solution using various kinds of layered double hydroxides. Catal Today. doi:10.1016/j.cattod.2014.09.005
17. Xu C, Gao Y, Liu X, Xin R, Wang Z (2013) Hydrotalcite reconstructed by *in situ* rehydration as a highly active solid base catalyst and its application in aldol condensations. RSC Adv 3:793–801
18. Abelló S, Medina F, Tichit D, Pérez-Ramírez J, Groen JC, Sueiras JE, Salagre P, Cesteros Y (2005) Chem Eur J 11:728–739
19. Huang L, Chu S, Wang J, Kong F, Luo L, Wang Y, Zou Z (2013) Novel visible light driven Mg–Zn–In ternary layered materials for photocatalytic degradation of methylene blue. Catal Today 212:81–88
20. Shao M, Han J, Wei M, Evans DG, Duan X (2011) The synthesis of hierarchical Zn–Ti layered double hydroxide for efficient visible-light photocatalysis. Chem Eng J 168:519–524
21. Xia SJ, Liu FX, Ni ZM, Xue JL, Qian PP (2013) Layered double hydroxides as efficient photocatalysts for visible-light degradation of Rhodamine B. J Colloid Interface Sci 405:195–200
22. Mohapartra L, Parida KM (2012) Zn–Cr layered double hydroxide: visible light responsive photocatalyst for photocatalytic degradation of organic pollutants. Sep Purif Technol 91:73–80
23. Sun J, Zhang Y, Cheng J, Fan H, Zhu J, Wang X, Ai S (2014) Synthesis of Ag/AgCl/Zn-Cr LDHs composite with enhanced visible-light photocatalytic performance. J Mol Catal A Chem 382:146–153
24. Chen G, Qian S, Tu X, Wei X, Zou J, Leng L, Luo S (2014) Enhancement photocatalytic degradation of rhodamine B on nanoPtintercalated Zn–Ti layered double hydroxides. Appl Surf Sci 293:345–351
25. Mohapatra L, Parida KM (2014) Dramatic activities of vanadate intercalated bismuth doped LDH for solar light photocatalysis. Phys Chem Chem Phys 16:16985–16996
26. Valente JS, Tzompantzi F, Prince J (2011) Highly efficient photocatalytic elimination of phenol and chlorinated phenols by CeO_2/MgAl layered double hydroxides. Appl Catal B Environ 102:276–285
27. Paušová Š, Krýsa J, Jirkovský J, Mailhot G, Prevot V (2012) Photocatalytic behavior of nanosized TiO_2 immobilized on layered double hydroxides by delamination/restacking process. Environ Sci Pollut Res 19:3709–3718
28. Yuan S, Li Y, Zhang Q, Wang H (2009) ZnO nanorods decorated calcined Mg–Al layered double hydroxides as photocatalysts with a high adsorptive capacity. Colloids Surf A 348:76–81
29. Dvininov E, Ignat M, Barvinschi P, Smithers MA, Popovici E (2010) New SnO_2/MgAl-layered double hydroxide composites as photocatalysts for cationic dyes bleaching. J Hazard Mater 177:150–158
30. Chen D, Li Y, Zhang J, Zhou JZ, Guo Y, Liu H (2012) Magnetic Fe_3O_4/ZnCr-layered double hydroxide composite with enhanced adsorption and photocatalytic activity. Chem Eng J 185–186:120–126
31. Guo Y, Li D, Hu C, Wang Y, Wang E, Zhou Y, Feng S (2001) Photocatalytic degradation of aqueous organocholorine pesticide on the layered double hydroxide pillared by Paratungstate A ion, $Mg_{12}Al_6(OH)_{36}(W_7O_{24})\cdot 4H_2O$. Appl Catal B Environ 30:337–349
32. Li B, Zhao Y, Zhang S, Gao W, Wei M (2013) Visible-light-responsive photocatalysts toward water oxidation based on NiTi-layered double hydroxide/reduced graphene oxide composite materials. ACS Appl Mater Interfaces 5:10233–10239

33. Zhao Y, Chen P, Zhang B, Su DS, Zhang S, Tian L, Lu J, Li Z, Cao X, Wang B, Wei M, Evans DG, Duan X (2012) Highly dispersed TiO_6 units in a layered double hydroxide for water splitting. Chem Eur J 18:11949–11958
34. Hong J, Wang Y, Pan J, Zhong Z, Xu R (2011) Self-assembled dye-layered double hydroxide-Pt nanoparticles: a novel H_2 evolution system with remarkably enhanced stability. Nanoscale 3:4655–4661
35. Teramura K, Tanaka T, Ishikawa H, Kohno Y, Funabiki T (2004) Photocatalytic reduction of CO_2 to CO in the presence of H_2 or CH_4 as a reductant over MgO. J Phys Chem B 108:346–354
36. Ahmed N, Shibata Y, Taniguchi T, Izumi Y (2011) Photocatalytic conversion of carbon dioxide into methanol using zinc–copper–M(III) (M = aluminum, gallium) layered double hydroxides. J Catal 279:123–135
37. Morikawa M, Ahmed N, Yoshida Y, Izumi Y (2014) Photoconversion of carbon dioxide in zinc–copper–gallium layered double hydroxides: the kinetics to hydrogen carbonate and further to CO/methanol. Appl Catal B Environ 144:561–569
38. Morikawa M, Ogura Y, Ahmed N, Kawamura S, Mikami G, Okamoto S, Izumi Y (2014) Photocatalytic conversion of carbon dioxide into methanol in reverse fuel cells with tungsten oxide and layered double hydroxide photocatalysts for solar fuel generation. Catal Sci Technol 4:1644–1651
39. Katsumata K, Sakai K, Ikeda K, Carja G, Matsushita N, Okada K (2013) Preparation and photocatalytic reduction of CO_2 on noble metal (Pt, Pd, Au) loaded Zn–Cr layered double hydroxides. Mater Lett 107:138–140
40. Teramura K, Iguchi S, Mizuno Y, Shishido T, Tanaka T (2012) Photocatalytic conversion of CO_2 in water over layered double hydroxides. Angew Chem Int Ed 51:8008–8011
41. Iguchi S, Teramura K, Hosokawa S, Tanaka T (2015) Effect of the chloride ion as a hole scavenger on the photocatalytic conversion of CO_2 in an aqueous solution over Ni–Al layered double hydroxides. Phys Chem Chem Phys 17:17995–18003